THE JOURNAL OF BIOLOGICAL CHEMISTRY VOL. 283, NO. 22, pp. 15328–15338, May 30, 2008

Noonan Syndrome-associated SHP-2/*Ptpn11* Mutants Enhance SIRPα and PZR Tyrosyl Phosphorylation and Promote Adhesion-mediated ERK Activation*

Received for publication, February 21, 2008, and in revised form, March 27, 2008 Published, JBC Papers in Press, March 31, 2008, DOI 10.1074/jbc.M801382200

Seda Eminaga and Anton M. Bennett[1]

From the Department of Pharmacology, Yale University School of Medicine, New Haven, Connecticut 06520

Noonan syndrome (NS) is an autosomal dominant disorder that is associated with multiple developmental abnormalities. Activated mutations of the protein-tyrosine phosphatase, SHP-2/*PTPN11*, have been reported in ~50% of NS cases. Despite being activated, NS-associated SHP-2 mutants require plasma membrane proximity to evoke disease-associated signaling. Here we show that NS-associated SHP-2 mutants induce hypertyrosyl phosphorylation of the transmembrane glycoproteins, SIRPα (signal-regulatory protein α) and PZR (protein zero-related), resulting in their increased association with NS-associated SHP-2 mutants. NS-associated SHP-2 mutants enhanced SIRPα and PZR tyrosyl phosphorylation either by impairing SIRPα dephosphorylation or by promoting PZR tyrosyl phosphorylation. Importantly, during embryogenesis in a mouse model of NS, SIRPα and PZR were hypertyrosyl-phosphorylated and bound increased levels of the NS-associated SHP-2 mutant. SIRPα and PZR have been implicated in extracellular matrix-dependent signaling. Mouse embryonic fibroblasts derived from a mouse model of NS displayed enhanced ERK activation in response to fibronectin plating. Knockdown of SIRPα and PZR in these cells attenuated the enhanced activation of ERK following fibronectin plating. Thus, SIRPα and PZR serve as scaffolds that facilitate plasma membrane recruitment and signaling of NS-associated SHP-2 mutants.

The Src homology 2 (SH2)[2] domain-containing protein-tyrosine phosphatase (PTP), SHP-2, is a ubiquitously expressed cytoplasmic PTP with two NH_2-terminal SH2 domains and a COOH-terminal PTP domain (1, 2). SHP-2, in most cases, is a positive transducer of growth factor, cytokine, integrin, and hormone signaling pathways regulating processes such as cell proliferation, differentiation, adhesion, migration, and apoptosis (1, 2). In virtually all cases, the catalytic activity of SHP-2 is required for its positive signaling effects that are mediated through the dephosphorylation of substrates that are negatively regulated by tyrosine phosphorylation (1–3). Either mutation or disruption of SHP-2 results in embryonic lethality in mice (4, 5). During embryogenesis, SHP-2 is required for mammalian limb development (6) and heart valvulogenesis (7). Hence, SHP-2 plays an essential role in mammalian development.

SHP-2 is the protein product of the *PTPN11* gene that is mutated in ~50% of Noonan syndrome (NS) cases (8, 9). NS is an autosomal dominant disorder that is estimated to occur in 1:1,000 to 1:2,500 live births in the United States and worldwide (9–11). NS patients are characterized by proportionate short stature, facial dysmorphisms, mental retardation, bleeding diathesis, and cardiovascular defects such as pulmonary stenosis (9–11). In addition, NS patients display hematologic abnormalities, including myeloid disorders and juvenile myelomonocytic leukemia (9). Most of the disease-associated mutations of SHP-2 have been mapped to the NH_2-SH2 domain, whereas other mutations map to either the COOH-SH2 or the PTP domain (8, 12, 13). SHP-2 is maintained in an "inactive" autoinhibited conformation that is maintained by interactions between the NH_2-SH2 domain and the PTP domain (14). Mutations within the SH2-PTP domain interface disrupt intramolecular interactions between these two domains to relieve the autoinhibited conformation resulting in constitutive SHP-2 activation (15). Several NS/leukemia-associated SHP-2 mutants are activating, hence conferring gain-of-function properties to SHP-2 (8, 12, 16–20). These observations support the notion that enhanced SHP-2 catalysis is causative to NS and leukemia.

It is now established that in response to a variety of growth factors and cytokines SHP-2 is required for the activation of Src (21–23), Ras/ERK (5, 24–26), and phosphatidylinositol 3′-kinase/Akt pathways (27–29). In addition, SHP-2 is also responsible for mediating the activation of the Src and Ras/ERK pathways following integrin engagement (21, 30, 31). In response to growth factors and cytokines, the gain-of-function properties of the NS/leukemia-associated SHP-2 mutants enhance ERK activation (17–19, 32–34). However, in some cases the NS/leukemia-associated SHP-2 mutants fail to enhance ERK activation (18, 35, 36). Such differences might reflect cell type-specific and possibly stimulation-dependent variations in which the NS/leukemia-associated SHP-2 mutants operate. Activated

* This work was supported, in whole or in part, by National Institutes of Health Grant R01 AR46504 (to A. M. B.). The costs of publication of this article were defrayed in part by the payment of page charges. This article must therefore be hereby marked "*advertisement*" in accordance with 18 U.S.C. Section 1734 solely to indicate this fact.

[1] To whom correspondence should be addressed: Dept. of Pharmacology, Yale University School of Medicine, SHM B226D, 333 Cedar St., New Haven, CT 06520-8066. Tel.: 203-737-2441; Fax: 203-737-2738; E-mail: anton.bennett@yale.edu.

[2] The abbreviations are: SH2, Src homology domain 2; ERK, extracellular signal-regulated kinases; Gab, Grb2-associated binder; MEFs, mouse embryo fibroblasts; NS, Noonan syndrome; SFK, Src family kinase; FBS, fetal bovine serum; WT, wild type; siRNA, small interfering RNA; DMEM, Dulbecco's modified Eagle's medium; EGF, epidermal growth factor; PDGF, platelet-derived growth factor; FGF-2, fibroblast growth factor-2; BSA, bovine serum albumin; PBS, phosphate-buffered saline; PTP, protein-tyrosine phosphatase; GST, glutathione *S*-transferase; GFP, green fluorescent protein.

and NS-associated SHP-2 mutants have also been shown to increase the calcium oscillatory frequency in fibroblasts and cardiomyocytes, and this correlates with the inhibition of the nuclear factor of activated T-cells in cardiomyocytes (37). In addition, the leukemia-associated mutants of SHP-2 also exhibit enhanced Akt activity (19, 33).

Despite a growing number of signaling pathways that are subject to altered regulation by NS/leukemia-associated SHP-2 mutants, the mechanism through which these activated SHP-2 mutations enhance downstream signaling remains to be fully defined. One mechanism through which activated SHP-2 mutants might enhance signaling is by increasing the levels of tyrosyl phosphorylation of their upstream interacting proteins and hence their association and recruitment to locales where signaling is initiated. We first showed that an activated SHP-2 mutant increases tyrosyl phosphorylation of the fibroblast growth factor receptor substrate-2 in response to FGF-2 (38). Similar observations with activated SHP-2 mutants were also found to occur with the Grb2-associated binder-1 (Gab-1), which becomes hypertyrosyl-phosphorylated in response EGF (17). As predicted, enhanced tyrosyl phosphorylation of SHP-2-binding proteins results in their increased association with SHP-2 (17, 18, 33). These observations suggest that binding and thus localization of the NS/leukemia-associated SHP-2 mutants play an important role in disease-mediated signaling. This notion is supported by the observation that disruption of Gab-2 binding by mutation of the critical arginine within the SH2 domain of the leukemogenic E76K SHP-2 mutant abrogates cellular transformation (19).

In this study, we show that NS/leukemia-associated SHP-2 mutants interact with, and induce hypertyrosyl phosphorylation of, the transmembrane glycoproteins SIRPα (signal regulatory protein α) and PZR (protein zero-related). We show that in mice harboring an NS-associated SHP-2 mutant, both SIRPα and PZR are hypertyrosyl-phosphorylated. Fibroblasts derived from these mice also exhibited increased SIRPα and PZR tyrosyl phosphorylation. The enhanced ERK activation in response to adhesion was predominantly mediated by SIRPα, with PZR playing less of a role. These results raise the possibility that SIRPα and PZR serve as scaffold proteins for NS/leukemia-associated mutants and may thus play a role in the pathogenesis of these diseases.

EXPERIMENTAL PROCEDURES

Cell Lines and Cell Culture—WT and D61G mouse embryonic fibroblasts (MEFs) were provided by Dr. Benjamin Neel (Beth Israel Deaconess Medical Center, Boston). C2C12 and $Src^{-/-}/Yes^{-/-}/Fyn^{-/-}$ (SYF) cells were purchased from ATCC. Cells were cultured at 37 °C in 5% CO_2 in Dulbecco's modified Eagle's medium (DMEM) (Invitrogen) containing 15% fetal bovine serum (FBS) (Sigma) for WT and D61G MEFs or 10% FBS for C2C12 and SYF cells containing 1 mM sodium pyruvate (Invitrogen), 5 units/ml penicillin, and 50 μg/ml streptomycin (Sigma). Insulin-like growth factor-1, EGF, FGF-2, and platelet-derived growth factor (PDGF) were purchased from Calbiochem. All chemicals are purchased from Sigma unless indicated otherwise.

Plasmids and Primers—pIRES-GFP expression plasmids encoding WT SHP-2 and Glu-76 to Ala-76 (E76A) were described previously (38). SHP-2 containing mutations at Asp-61 to Ala-61 (D61A), Glu-69 to Lys-69 (E69K), Asn-308 to Asp-308 (N308D), and E76A containing an Arg-465 to Met-465 (R465M/E76A) mutation were generated by site-directed mutagenesis and verified by automated sequencing. The tandem NH_2 and COOH-SH2 domains (amino acids 1–215) were subcloned into a GST fusion expression vector (pEBG) to generate pEBG-SH2 by PCR using BamHI and NotI with the primers 5′-CGC GGA TCC ATG ACA TCG CGG AGA TGG-3′ and 5′-ATA GTT TAG CGG CCG CTC AGG GCT GCT TGA GTT GTA G-3′. Mammalian plasmids expressing PZR (pCDNA3-PZR-WT) and SIRPα (pJ3-SIRPα) were provided by Dr. Joe Zhao (University of Oklahoma, Oklahoma City) and Dr. Benjamin Neel (Beth Israel Deaconess Medical Center, Boston), respectively. Mice were genotyped as described previously (18).

Adenoviral Infections—Replication-defective recombinant WT and activated E76A SHP-2 adenoviruses have been described previously (38). Adenoviruses were amplified in 293 cells and purified according to the manufacturer's instructions (Quantum-Appligene).

Transient Transfections—C2C12 cells were transfected with the indicated plasmids using Lipofectamine 2000 (Invitrogen), and SYF cells were transfected using FuGENE transfection reagent according to the manufacturer's instructions (Roche Applied Science). For siRNA transfections, 100,000 MEFs derived from the D61G NS knock-in mice (18) were plated onto 60-mm tissue culture plates 1 day prior to transfection and were transfected with either 50 nM SIRPα siRNA (Santa Cruz Biotechnology), 25 nM PZR siRNA (Dharmacon), or control nontargeting siRNA (Dharmacon and/or Santa Cruz Biotechnology) using Lipofectamine RNAiMAX reagent (Invitrogen) according to the manufacturer's instructions. 24 h after transfection cells were serum-deprived (0.1% FBS/DMEM) overnight, and the cells were trypsinized for re-plating onto fibronectin-coated Petri dishes.

Immunoprecipitations and Immunoblot Analyses—Cells were lysed on ice in 1% Nonidet P-40 buffer (Calbiochem) containing 150 mM NaCl, 50 mM Tris-HCl, pH 7.4, 5 mM EDTA, 1% Nonidet P-40, 1 mM Na_3VO_4, 10 mM NaF, 1 mM benzamidine, 1 mM PMSF, 1 μg/ml pepstatin A, 5 μg/ml aprotinin, and 5 μg/ml leupeptin. Where indicated cells were lysed in modified radioimmunoprecipitation assay buffer, containing 1% Nonidet P-40 lysis buffer supplemented with 1% sodium deoxycholate and 0.1% SDS. E12.5–14.5 embryos were obtained from timed pregnancies and lysed by homogenizing (20 strokes) in 1% Triton X-100, 0.1% SDS, 0.5% sodium deoxycholate, 20 mM HEPES, pH 7.4, 150 mM NaCl, 10% glycerol, 2 mM EDTA, 10 mM NaF, 1 mM Na_3VO_4, 1 mM PMSF, 1 mM dithiothreitol, 1 mM benzamidine, 1 μg/ml pepstatin A, 5 μg/ml leupeptin, and 5 μg/ml aprotinin. Cell or embryo lysates were rocked at 4 °C for 15–20 min and clarified by centrifugation at 20,800 $\times$ *g* at 4 °C for 20 min. Protein concentration was determined using the Bradford assay or BCA reagent according to the manufacturer's instructions (Pierce). For immunoprecipitations, 500–1,000 μg of lysate was incubated with 4 μg of SHP-2 polyclonal antibody

(Santa Cruz Biotechnology), 1 μl of PZR polyclonal antibody (antisera 105(6) or 189(14) provided by Dr. Joe Zhao), 2 μl of SIRPα polyclonal antibody (provided by Dr. Benjamin Neel), and 2 μg of Src (GD11) monoclonal antibody (BD Transduction Laboratories) for 3 h or overnight at 4 °C. Immune complexes were collected on either protein A- or G-Sepharose (GE Healthcare). Immune complexes were washed three times with either 1% Nonidet P-40 or Triton X-100 lysis buffer containing 1 mM Na_3VO_4 and 10 mM NaF and once with STE buffer (100 mM NaCl, 10 mM Tris-HCl, pH 8.0, 1 mM EDTA), and beads were heated to 95 °C in sample buffer (62.5 mM Tris, pH 6.8, 4% glycerol, 2% SDS, 5% β-mercaptoethanol, and 0.02% bromphenol blue) for 5 min.

For immunoblotting, lysates or immune complexes were resolved by SDS-PAGE and transferred onto Immobilon-P membranes (Millipore). All primary antibodies were used by first blocking membranes with 5% nonfat dry milk or 5% BSA in Tris-buffered saline/Tween 20 (TBS-T) for 1 h at room temperature or overnight at 4 °C. Primary antibodies were diluted in 2.5% nonfat dried milk in TBS-T or 2.5% BSA in TBS-T. Mouse monoclonal SHP-2 antibody (BD Transduction Laboratories) was used at a 1:1,000 dilution. Anti-PZR antibody (105(6)) was used at a 1:5,000 dilution. SIRPα polyclonal antibody was used at a 1:5,000 dilution; monoclonal anti-phosphotyrosine (4G10) antibody was used at a 1:50 dilution; rabbit polyclonal phospho-p44/42 MAPK antibody (Cell Signaling Technology) was used at a 1:1,000 dilution; and rabbit polyclonal ERK1/2 (Santa Cruz Biotechnology) antibody was used at a 1:4,000 dilution. Monoclonal c-Src (GD11, Upstate Biotechnology, Inc.) antibody was used at a 1:1,000 dilution, and polyclonal phospho-Src Tyr-416 antibody (Cell Signaling Technology) was used at a 1:500 dilution. Primary antibodies were either used at room temperature for 2 h or overnight at 4 °C. After primary antibody incubations, membranes were washed in TBS-T and incubated in secondary anti-rabbit Ig horseradish peroxidase-linked donkey antibody or anti-mouse Ig horseradish peroxidase-linked sheep antibody (GE Healthcare) for 1 h at room temperature. After secondary antibody incubations, membranes were washed in TBS-T and visualized by using enhanced chemiluminescence reagents (Amersham Biosciences).

Immune Complex Phosphatase Assays—C2C12 cells transfected with the indicated expression plasmids were lysed in 1% Nonidet P-40 lysis buffer 24 h after transfection, and cell lysates were subjected to immunoprecipitation with anti-SHP-2 polyclonal antibody overnight at 4 °C. Immune complexes were captured by incubation with protein A-Sepharose and were washed several times with lysis buffer containing 10 mM NaF, once with STE buffer, and once with phosphatase assay buffer (24 mM HEPES, pH 7.4, 120 mM NaCl). Phosphatase assay buffer containing 10 mM *para*-nitrophenyl phosphate and 5 mM dithiothreitol was added to the immune complexes and incubated at 37 °C for 30 min. Reactions were stopped by addition of 1.45 ml of 0.2 N NaOH, and the absorbance at 405 nm was measured.

Cell Adhesion Assays—Petri dishes were coated with fibronectin (5 μg/ml) diluted in PBS for 1–2 h at 37 °C and were blocked with 1% BSA in PBS for 30 min at 37 °C. WT and D61G MEFs or D61G MEFs treated with siRNA were serum-deprived overnight and were detached by 0.05% trypsin/EDTA and neutralized with 0.5 mg/ml soybean trypsin inhibitor solution in DMEM. Cells were washed in serum-free DMEM containing 0.1% BSA, held in suspension for 30 min at 37 °C under a humidified atmosphere containing 5% CO_2, and were re-plated (575,000 cells per 60-mm dish) onto either 1% BSA blocked Petri dishes (suspension) or fibronectin-coated Petri dishes. Cells were harvested at the indicated times by washing twice in ice-cold PBS and lysing as indicated above.

For quantification of adhesion, wells of a 96-well plate (Linbro-Titertek) were coated with the indicated concentrations of fibronectin in triplicate. Serum-deprived cells were trypsinized and washed in serum-free DMEM containing 0.1% BSA. 20,000 cells/well were plated and allowed to attach for 30 min at 37 °C. The attached cells were washed once with PBS, fixed in 4% paraformaldehyde solution in PBS for 20 min at room temperature, and stained with 0.5% crystal violet solution in 20% methanol for at least 1 h. Crystal violet was extracted with 10% acetic acid and was measured in a multiple well plate reader at 562 nm.

Cell Migration Assay—Migration of WT and D61G MEFs was quantified using a transwell migration assay. The bottom side of the transwell insert membrane (8 μm pore size, Costar) was coated with 5 μg/ml of fibronectin in triplicate at 37 °C for 1 h and blocked with 1% BSA solution. Cells were trypsinized and washed as described above, plated at a density of 5,000 cells per well, and allowed to migrate for 5 h in a humidified incubator at 37 °C. The cells that had migrated were washed once in PBS, fixed with 4% paraformaldehyde/PBS, and stained with 0.5% crystal violet solution. After the cells on top of the transwell insert membrane were scraped with cotton tips, the cells remaining on the bottom of the membrane were photographed in four fields/well using a 5× objective and cells were counted using NIH Image J software.

RESULTS

Enhanced Association of Tyrosyl-phosphorylated Proteins with Activated SHP-2 Mutants—SHP-2 engages in a complex complement of protein-protein interactions mediated by its SH2 domains that serve to both activate and target it to specific subcellular compartments (1). Despite being constitutively active, mutants of SHP-2 likely require appropriate subcellular localization, mediated through its SH2 domains, to promote disease-associated signaling (19). We therefore sought to identify tyrosyl-phosphorylated proteins that might serve as signaling scaffolds for activated SHP-2 mutants in an attempt to explore the signaling mechanisms involved in the pathogenesis of NS/leukemia.

We first began by generating four distinct activated SHP-2 mutants; the N308D mutation represents the most common mutation in NS (39); E69K and E76A mutations are associated with leukemia (39), and D61A is a molecular gain-of-function mutation (15) (Fig. 1*A*). These mutants were expressed transiently in C2C12 cells, and immune complex phosphatase assays were performed (Fig. 1*B*). Cells expressing these activated SHP-2 mutants, as expected (15, 16, 20, 35, 40), exhibited levels of phosphatase activity greater than that of WT overexpressing cells (Fig. 1*B*). The activated SHP-2 mutant expressing cells displayed varying levels of enhanced phosphatase activity

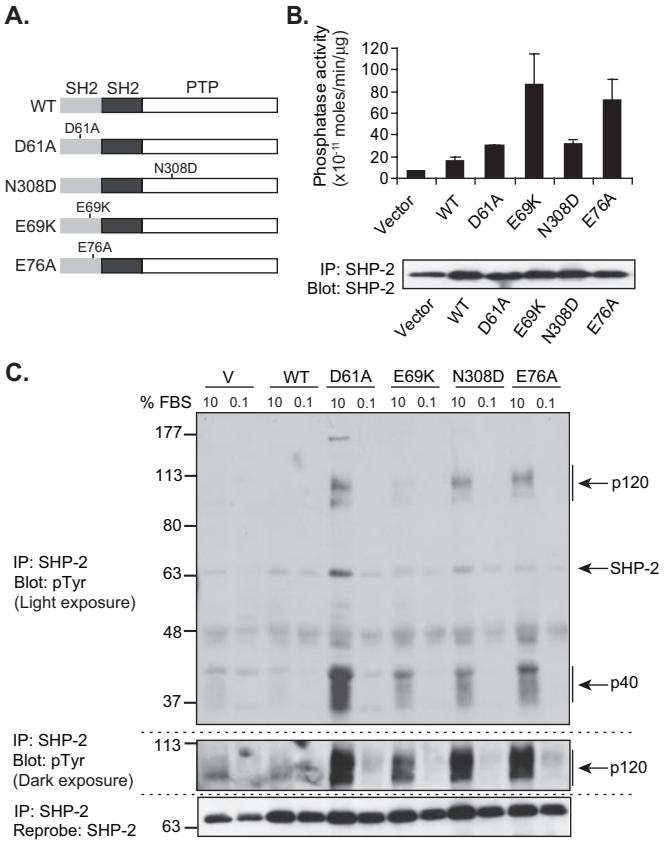

FIGURE 1. **Enhanced association of tyrosyl-phosphorylated proteins with gain-of-function and NS/leukemia-associated SHP-2.** *A,* schematic representation of NS/leukemia-associated SHP-2 mutants. *B, in vitro* phosphatase activity of activated SHP-2 mutants. Lysates derived from C2C12 cells transiently transfected with vector, SHP-2 WT, and activated SHP-2 mutants (D61A, E69K, N308D, and E76A) were subjected to immunoprecipitation (*IP*) with anti-SHP-2 antibodies, and immune complex phosphatase assays were performed. Data are representative of the mean ± S.E. from three separate experiments. SHP-2 immune complexes were resolved by SDS-PAGE and immunoblotted with anti-SHP-2 antibodies. *C,* cells transfected as in *B* were cultured in either 10 or 0.1% FBS, and lysates were subjected to immunoprecipitation with anti-SHP-2 antibodies, and immune complexes were resolved by SDS-PAGE and immunoblotted with anti-phosphotyrosine (*pTyr*) 4G10 antibodies (*upper panel*). A longer exposure representing the p120 immune complex is shown (*middle panel*). Immunoblots were re-probed with anti-SHP-2 antibodies (*lower panel*). *V*, vector.

with a rank order of E69K ≥ E76A > N308D ≥ D61A (Fig. 1*B*). Next, C2C12 cells cultured either under 10% FBS or 0.1% FBS conditions were transiently transfected with WT, D61A, N308D, or E76A activated SHP-2 mutants, and SHP-2 immune complexes derived from these cell lysates were immunoblotted with anti-phosphotyrosine antibodies (Fig. 1*C*). Cells expressing the activated SHP-2 mutants were found under proliferative conditions to interact with two tyrosyl-phosphorylated proteins that migrated with apparent molecular masses of 120 and 40 kDa, referred to herein as p120 and p40 proteins, respectively. In contrast, WT expressing cells failed to interact appreciably with either p120 or p40 tyrosyl-phosphorylated proteins (Fig. 1*C*). WT and SHP-2 activated mutants were comparably expressed (Fig. 1*C*), indicating that these activated SHP-2 mutants either enhance tyrosyl phosphorylation levels and/or interaction with the p120 and p40 tyrosyl-phosphorylated proteins.

SIRPα and PZR Are Targets for Hypertyrosyl Phosphorylation by Activated SHP-2 Mutants—We next set out to identify the SHP-2-associated p120 and p40 tyrosyl-phosphorylated proteins. Based on our previous observations, as well as those of others, we noted that the broad nature of the SHP-2-associated phosphotyrosyl p120 protein was reminiscent of the SHP-2-binding protein known as SIRPα, which also migrates with an apparent molecular mass between 110 and 120 kDa (41–44). SIRPα is a transmembrane glycoprotein containing three immunoglobulin-like domains extracellularly, and four tyrosine residues intracellularly, two of which exist in context of an immunoreceptor tyrosine-based inhibitory motif (45, 46). SIRPα was initially identified as a substrate and binding protein for SHP-2 (42, 43, 47), and it has been implicated in a number of signaling events, including the regulation of the extracellular-regulated kinases (ERKs) 1 and 2, cell motility, and adhesion-mediated integrin signaling (31, 46, 48, 49). We tested whether SIRPα constitutes a component of the SHP-2-associated tyrosyl-phosphorylated p120 protein upon expression of the activated SHP-2 mutants.

The activated SHP-2 mutant enhanced the association of SHP-2 with the p120 and p40 tyrosyl-phosphorylated proteins using adenovirus-mediated delivery to express WT and E76A (Fig. 2*A*). When immunoprecipitated, SIRPα was tyrosyl-phosphorylated to a greater extent in E76A as compared with WT expressing cells (Fig. 2*B*). We next determined whether SIRPα is, or constitutes a component of, the SHP-2-associated p120 tyrosyl-phosphorylated protein. To test this, we immunodepleted SIRPα from the lysates of cells infected with adenoviruses expressing GFP as a control, WT, or E76A followed by immunoprecipitation of SHP-2. When SIRPα was immunodepleted from these cell lysates followed by immunoprecipitation of SHP-2, the p120 tyrosyl-phosphorylated protein was depleted from these complexes as compared with the preimmune control immunodepletion (Fig. 2*C*). Both E76A and N308D SHP-2 mutants not only induced hypertyrosyl phosphorylation of SIRPα, but also this was accompanied by increased levels of associated SHP-2 (Fig. 2*D*). These data identify SIRPα as the major component of the SHP-2-associated tyrosyl-phosphorylated p120 protein in cells expressing an activated SHP-2 mutant.

Next, we sought to identify the SHP-2-associated p40 tyrosyl-phosphorylated protein. Although a number of tyrosyl-phosphorylated SHP-2-interacting proteins have been identified, one of these proteins migrates with a molecular mass of ~40 kDa and is known as PZR. Like SIRPα, PZR is also a transmembrane glycoprotein containing a single immunoglobulin-like domain extracellularly and two immunoreceptor tyrosine-based inhibitory motifs intracellularly (50). PZR was also shown to interact directly with SHP-2 and was suggested to be an SHP-2 substrate (51). To determine whether PZR constituted a component of the SHP-2-associated p40 tyrosyl-phosphorylated protein complex, C2C12 cells were infected with adenoviruses expressing GFP, WT, or E76A, and tyrosyl phosphorylation of PZR was determined. These experiments revealed that PZR was hypertyrosyl-phosphorylated in E76A as compared with WT expressing cells (Fig. 3*A*). We attempted to perform immunodepletion experiments to determine to what extent

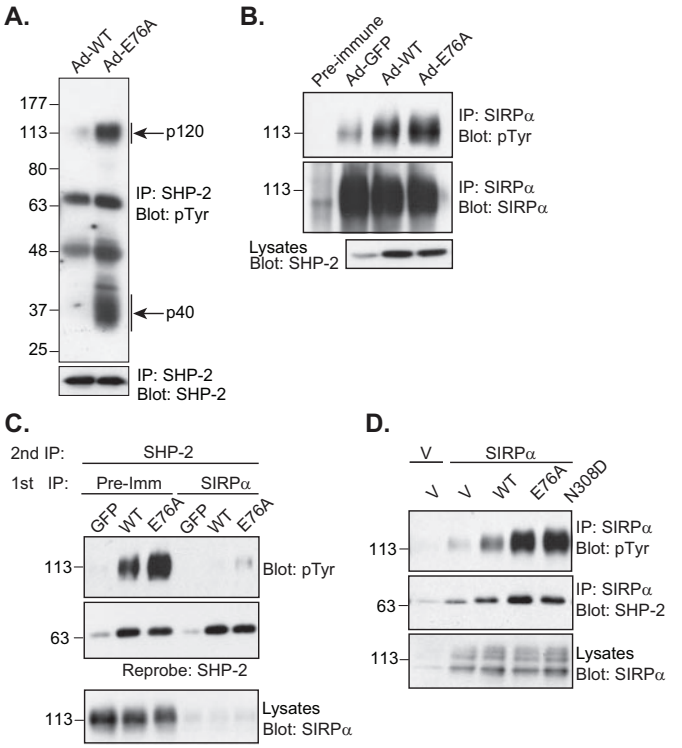

FIGURE 2. **SIRPα is a major component of the SHP-2-associated tyrosyl-phosphorylated p120 protein in cells expressing activated SHP-2.** *A,* lysates obtained from C2C12 cells infected with Ad-SHP-2 WT or Ad-SHP-2 E76A adenoviruses were subjected to immunoprecipitation (*IP*) with anti-SHP-2 antibodies; immune complexes were resolved by SDS-PAGE and immunoblotted with anti-Tyr(P) (*pTyr*) antibodies. Immunoblots were re-probed with anti-SHP-2 antibodies (*lower panel*). *B,* cell lysates derived from C2C12 cells infected as in *A* were subjected to immunoprecipitation with anti-SIRPα antibodies or preimmune sera, and immune complexes were immunoblotted with anti-Tyr(P) antibodies (*upper panel*) and anti-SIRPα antibodies (*middle panel*). SHP-2 expression levels in cell lysates are shown (*lower panel*). *C,* lysates derived from C2C12 cells infected as in *A* were immunoprecipitated with control preimmune (*Pre-Imm*) sera or anti-SIRPα antibodies. Supernatants following control or SIRPα immunoprecipitation were recovered and subjected to immunoprecipitation with anti-SHP-2 antibodies. Immune complexes were resolved by SDS-PAGE and immunoblotted with anti-Tyr(P) (*top panel*), anti-SHP-2 antibodies (*middle panel*), and cell lysates were immunoblotted with anti-SIRPα antibodies (*lower panel*). *D,* lysates obtained from C2C12 cells transiently co-transfected with vector (*V*), SHP-2 wild-type (*WT*), and the activated mutants N308D and E76A along with vector or SIRPα were subjected to immunoprecipitation with anti-SIRPα antibodies and immunoblotted with anti-Tyr(P) antibodies (*upper panel*) and anti-SHP-2 antibodies (*middle panel*). Lysates were immunoblotted with anti-SIRPα antibodies as a control for SIRPα expression levels (*lower panel*).

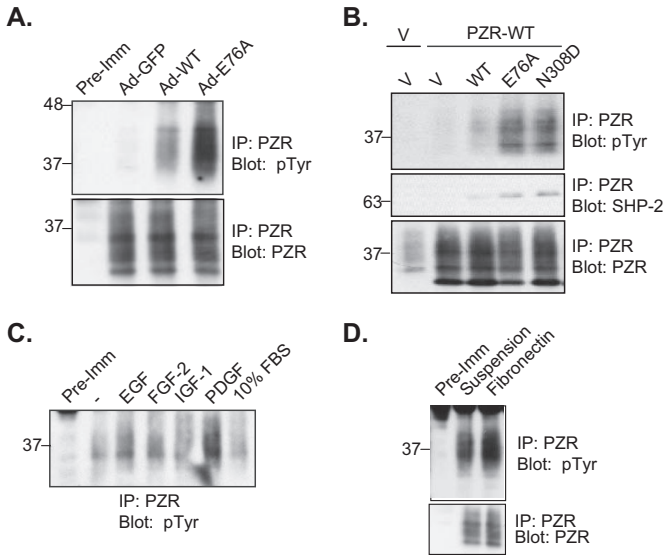

FIGURE 3. **Increased tyrosyl phosphorylation of PZR in cells expressing activated SHP-2.** *A,* lysates derived from C2C12 cells infected with control Ad-GFP, Ad-SHP-2 WT, and Ad-SHP-2 E76A were subjected to immunoprecipitation (*IP*) with either preimmune (*Pre-Imm*) sera or anti-PZR antibodies; immune complexes were resolved by SDS-PAGE and immunoblotted with anti-Tyr(P) (*pTyr*) antibodies (*upper panel*) and anti-PZR antibodies (*lower panel*). *B,* lysates derived from C2C12 cells transiently co-transfected with either vector (*V*), SHP-2 WT, N308D, or E76A along with vector or PZR-WT were subjected to immunoprecipitation with anti-PZR antibodies, and immune complexes were immunoblotted with either anti-Tyr(P) (*pTyr*) (*top panel*), anti-SHP-2 (*middle panel*), or anti-PZR (*bottom panel*) antibodies. *C,* C2C12 cells were serum-deprived for 16 h and stimulated with either EGF (10 ng/ml), FGF-2 (20 ng/ml), insulin-like growth factor-1 (50 ng/ml), PDGF (10 ng/ml), or 10% FBS for 10 min. Cell lysates were subjected to immunoprecipitation with anti-PZR antibodies, and immune complexes were immunoblotted with anti-Tyr(P) antibodies. *D,* C2C12 cells were trypsinized and were either kept in suspension or re-plated onto fibronectin-coated Petri dishes for 15 min. Lysates were subjected to immunoprecipitation with either preimmune sera or anti-PZR antibodies, and immune complexes were immunoblotted with either anti-Tyr(P) (*upper panel*) or anti-PZR antibodies (*lower panel*).

PZR contributed to the SHP-2-associated p40 complex. However, PZR antibodies were incapable of immunodepleting cell lysates of PZR effectively. Regardless, these results still suggest that at least a component of the SHP-2-associated p40 phosphotyrosyl protein is PZR. The ability of PZR to undergo enhanced association with SHP-2 upon expression of the activated SHP-2 mutants was evaluated. Transient expression of either N308D or E76A resulted in increased association of SHP-2 with PZR (Fig. 3*B*). Unlike SIRPα, where a number of reports have shown that it becomes tyrosyl-phosphorylated in response to growth factors, cytokines, and cell adhesion, the physiological stimuli that regulate PZR tyrosyl phosphorylation are unknown. When PZR was immunoprecipitated from cells that were stimulated with EGF, FGF-2, insulin-like growth factor-1, and serum, we found that it was not inducibly tyrosyl-phosphorylated, although a slight increase in PZR tyrosyl phosphorylation was observed in response to PDGF (Fig. 3*C*). In contrast, PZR was inducibly tyrosyl-phosphorylated upon fibronectin plating (Fig. 3*D*). These results demonstrate that PZR, like SIRPα, becomes tyrosyl-phosphorylated in response to adhesion-dependent signals.

SIRPα and PZR Are Targets for Enhanced Tyrosyl Phosphorylation and SHP-2 Recruitment in D61G Knock-in Mice—To determine whether SIRPα and/or PZR hypertyrosyl phosphorylation by activated SHP-2 mutants might have pathophysiological relevance to NS, we asked whether these transmembrane glycoproteins were hypertyrosyl-phosphorylated during embryogenesis in mice harboring a knock-in mutation of the NS-associated SHP-2 D61G mutation (18). Whole embryos were isolated from pregnant females between embryonic days 12.5 and 14.5. Extracts from WT and heterozygous (*Ptpn11*$^{D61G/+}$) embryos were subjected to immunoprecipitation for SHP-2, and the phosphatase activity was determined. The phosphatase activity of SHP-2 was ~3-fold more active in *Ptpn11*$^{D61G/+}$ embryos as compared with WT embryos (data not shown). Remarkably, SHP-2 co-immunoprecipitated with an identical profile of hypertyrosyl-phosphorylated associated proteins from *Ptpn11*$^{D61G/+}$ embryos as in transient cell culture experiments (Fig. 4*A*).

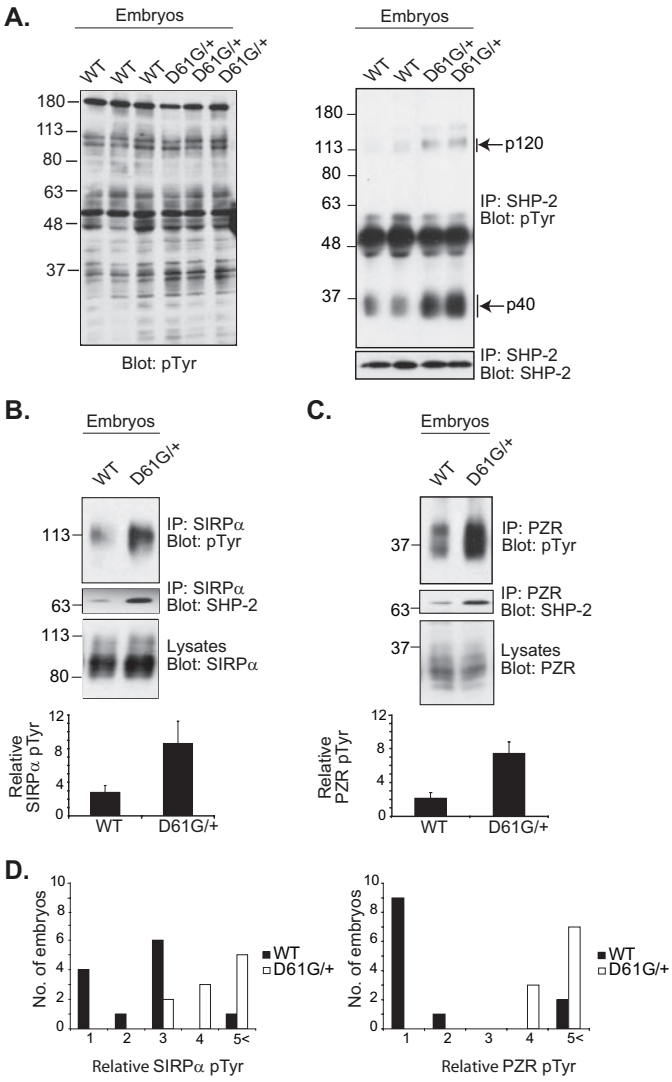

FIGURE 4. **SIRPα and PZR are hypertyrosyl-phosphorylated in *Ptpn11*$^{D61G/+}$ embryos.** *A,* whole embryos (WT and *Ptpn11*$^{D61G/+}$) were isolated from pregnant females between E12.5 and E14.5 days, and extracts were prepared and immunoblotted with anti-Tyr(P) (*pTyr*) antibodies (*left panel*). Extracts were subjected to immunoprecipitation (*IP*) with anti-SHP-2 antibodies, and immune complexes were immunoblotted with anti-Tyr(P) antibodies (*right panel*). The immunoblot was stripped and re-probed with anti-SHP-2 antibodies. Embryo extracts were prepared and subjected to immunoprecipitation with anti-SIRPα (*B*) or anti-PZR antibodies (*C*), and immune complexes were immunoblotted with anti-Tyr(P) and anti-SHP-2 antibodies. Lysates in *B* and *C* were immunoblotted with anti-SIRPα and anti-PZR antibodies. Densitometric analysis of tyrosyl phosphorylation levels of SIRPα and PZR in WT ($n = 12$) and *Ptpn11*$^{D61G/+}$ ($n = 10$) embryos normalized to total SIRPα (*B*) and PZR protein (*C*) in lysates. *D,* distribution levels of tyrosyl-phosphorylated SIRPα and PZR in WT and *Ptpn11*$^{D61G/+}$ embryos.

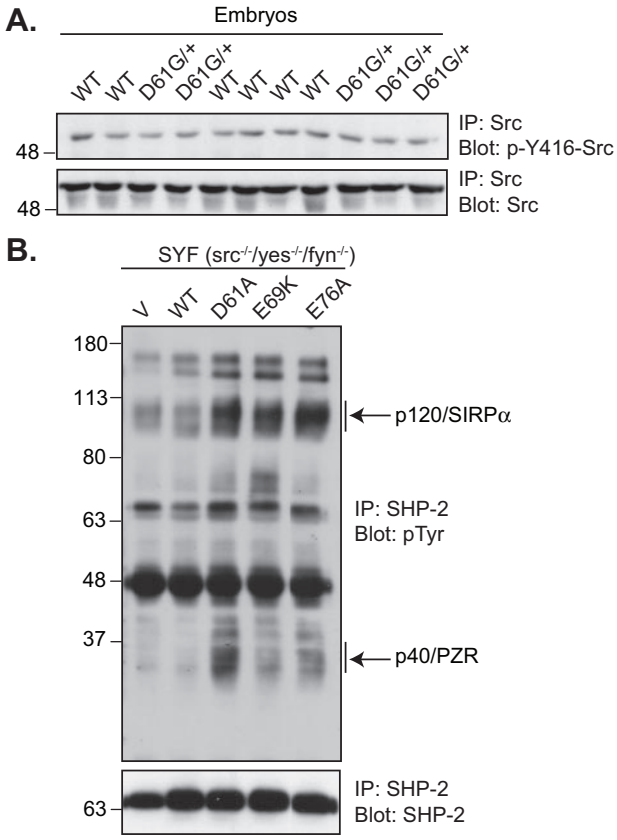

FIGURE 5. **c-Src activity is unaffected in D61G NS mice.** *A,* whole embryos (WT and *Ptpn11*$^{D61G/+}$) were isolated from pregnant females between days E12.5 and E14.5, and extracts were prepared and subjected to immunoprecipitation (*IP*) with anti-Src antibodies. Immune complexes were immunoblotted with anti-phospho-Y416-Src (*upper panel*) and anti-Src antibodies (*lower panel*). *B,* lysates derived from SYF cells transiently transfected with vector, SHP-2 WT, and activated mutants (D61A, E69K, and E76A) were subjected to immunoprecipitation with anti-SHP-2 antibodies. Immune complexes were immunoblotted with anti-Tyr(P) (*pTyr*) antibodies (*upper panel*) and re-probed with anti-SHP-2 antibodies.

Moreover, SIRPα and PZR were hypertyrosyl-phosphorylated, and this correlated with enhanced SHP-2 binding in *Ptpn11*$^{D61G/+}$ embryos as compared with WT embryos (Fig. 4, *B* and *C*). We quantitated the levels of SIRPα and PZR tyrosyl phosphorylation in individual WT and *Ptpn11*$^{D61G/+}$ embryos (Fig. 4*D*). This analysis showed an increase in the distribution of *Ptpn11*$^{D61G/+}$ embryos expressing elevated levels of tyrosyl-phosphorylated SIRPα (Fig. 4*D*, *left panel*) and PZR (Fig. 4*D*, *right panel*) as compared with WT embryos. These results demonstrate that SIRPα and PZR are hypertyrosyl-phosphorylated *in vivo* and constitute preferential SHP-2-interacting proteins during embryogenesis in *Ptpn11*$^{D61G/+}$ knock-in mice.

Activated SHP-2 Mutants Induce SIRPα and PZR Hypertyrosyl Phosphorylation in a c-Src-independent Manner—SHP-2 has been shown to be upstream of the Src family kinases (SFKs) (5, 21–23). In addition, both SIRPα and PZR contain immunoreceptor tyrosine inhibitory motifs, which are established SFK substrate motifs. Therefore, the activated SHP-2 mutants might induce SIRPα and PZR tyrosyl phosphorylation by activating the SFKs. Therefore, we determined whether c-Src activity is increased in *Ptpn11*$^{D61G/+}$ embryos. Whole embryo lysates were prepared from WT and *Ptpn11*$^{D61G/+}$ embryos, and c-Src Tyr-416 phosphorylation, which is representative of the active form of c-Src, was determined. We found that c-Src phosphorylation levels were unaltered in *Ptpn11*$^{D61G/+}$ embryos as compared with WT embryos (Fig. 5*A*). These results demonstrate that c-Src is unlikely to be a major target of the D61G NS mutant during embryogenesis that is responsible for either SIRPα or PZR tyrosyl phosphorylation. However, this result does not exclude the possibility that more discrete tissue-specific activation of the SFKs in *Ptpn11*$^{D61G/+}$ mice occurs. Another possibility is that SFKs other than c-Src might be tar-

gets for activated SHP-2 mutants that mediate SIRPα and PZR tyrosyl phosphorylation. To test other SFK members, fibroblasts lacking Src, Yes, and Fyn (SYFs) were transiently transfected with vector, WT, and three activated SHP-2 mutants. We found that all activated SHP-2 mutants were still capable of enhancing tyrosyl phosphorylation of the SHP-2-associated p120/SIRPα and p40/PZR proteins (Fig. 5*B*). Hence, the activated SHP-2 mutants appear to induce SIRPα and PZR hypertyrosyl phosphorylation in a c-Src-independent manner.

Distinct Mechanisms of SIRPα and PZR Hypertyrosyl Phosphorylation by Activated SHP-2 Mutants—One possible explanation for why the activated SHP-2 mutants induced hypertyrosyl phosphorylation of SIRPα and PZR could be related to the open conformation of these mutants. When activated, the open conformation of SHP-2 is presumed to have increased availability to bind through its SH2 domains to tyrosyl-phosphorylated proteins resulting in their protection from dephosphorylation. To examine this possibility, we engineered a catalytically inactive/nonsubstrate-trapping SHP-2 mutant (R465M) in context of the E76A mutation to generate a compound SHP-2 mutant (E76A/R465M) that is catalytically inactive but resides in an open conformation. C2C12 cells were transfected with either vector, WT, E76A, or E76A/R465M along with plasmids expressing either SIRPα or PZR. As expected, expression of E76A resulted in the hypertyrosyl phosphorylation of both SIRPα and PZR (Fig. 6, *A* and *B*). Interestingly, expression of E76A/R465M also induced hypertyrosyl phosphorylation of SIRPα and PZR (Fig. 6, *A* and *B*). There are two possible interpretations of these data. The first is that hypertyrosyl phosphorylation of SIRPα and PZR might occur because of a protective effect of the SHP-2 SH2 domains. Hence, the catalytic activity of the activated SHP-2 mutant might be dispensable for SIRPα and PZR hypertyrosyl phosphorylation. The second possibility is that because both SIRPα and PZR are putative SHP-2 substrates, overexpression of a catalytically inactive mutant of SHP-2 could also result in their hypertyrosyl phosphorylation (47, 51).

If the SH2 domains of the activated SHP-2 mutants simply protected SIRPα and PZR from dephosphorylation, expressing the SH2 domains of SHP-2 alone would result in the hypertyrosyl phosphorylation of SIRPα and PZR. However, if SHP-2 catalysis and/or adaptor function were required for SIRPα and PZR hypertyrosyl phosphorylation, the SH2 domains when overexpressed should function as a dominant-negative mutant of SHP-2 (26, 52) and suppress SIRPα and PZR hypertyrosyl phosphorylation. To distinguish between these possibilities, C2C12 cells were transiently co-transfected with GST fusions of WT, N308D, E76A, and the SH2 domains alone of SHP-2 (SH2) along with either full-length SIRPα or PZR. When the tandem SH2 domains of SHP-2 were expressed in cells and the status of SIRPα tyrosyl phosphorylation was examined, we found that SIRPα tyrosyl phosphorylation was induced to levels equivalent to that of cells expressing either E76A or N308D (Fig. 6*C*). These results imply that SIRPα hypertyrosyl phosphorylation is likely caused by the SH2 domains of SHP-2 binding to, and subsequently protecting, SIRPα from dephosphorylation. In contrast, we found that PZR tyrosyl phosphorylation was suppressed by the SH2 domains of

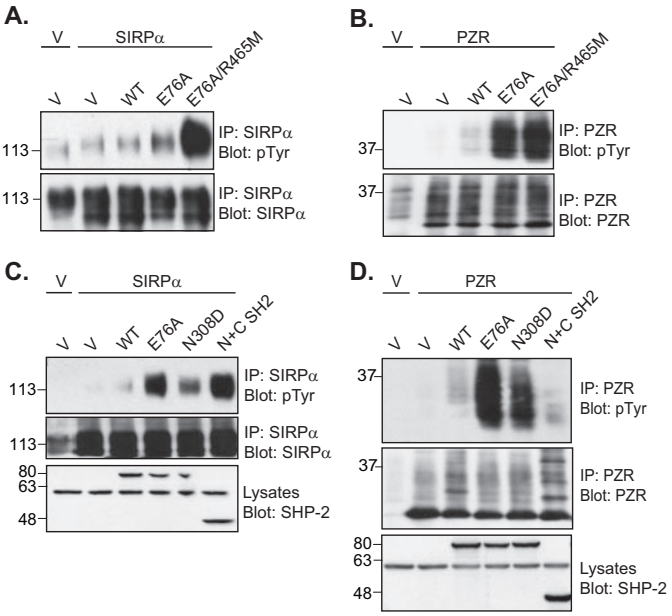

FIGURE 6. **Distinct modes of SIRPα and PZR hypertyrosyl phosphorylation by activated SHP-2.** C2C12 cells were transiently co-transfected with vector (*V*), SHP-2 WT, E76A and E76A/R465M along with either SIRPα (*A*) or PZR (*B*). Cell lysates were subjected to immunoprecipitation (*IP*) with anti-SIRPα (*A*) or anti-PZR antibodies (*B*), and immune complexes were resolved by SDS-PAGE and immunoblotted with anti-Tyr(P) (*pTyr*) antibodies. *C,* C2C12 cells were transiently co-transfected with pEBG vector (GST alone), GST-SHP-2 WT, N308D, E76A, N+C-SH2 domains, and SIRPα. Cell lysates were subjected to immunoprecipitation with anti-SIRPα antibodies, and immune complexes were immunoblotted with either anti-Tyr(P) (*upper panel*) or anti-SIRPα (*middle panel*) antibodies. SH2 domain expression was assessed by immunoblotting cell lysates with anti-SHP-2 antibodies (*lower panel*). *D,* cells were transfected with the plasmids indicated in *C* except that SIRPα was replaced with PZR. Cell lysates were subjected to immunoprecipitation with anti-PZR antibodies, and immune complexes were immunoblotted with either anti-Tyr(P) (*upper panel*) or anti-PZR (*middle panel*) antibodies. SH2 domain expression was assessed by immunoblotting cell lysates with anti-SHP-2 antibodies (*lower panel*).

SHP-2 (Fig. 6*D*). The SH2 domains were expressed to levels that were comparable with WT and activated SHP-2 mutants (Fig. 6, *C* and *D*). These results indicate that, unlike SIRPα, hypertyrosyl phosphorylation of PZR induced by the activated SHP-2 mutants is not a result of a protection effect by the SH2 domains. Therefore, in context of full-length activated SHP-2 mutants, PZR hypertyrosyl phosphorylation is presumably promoted either through the PTP domain of SHP-2 and/or an adaptor mechanism through its COOH terminus. Collectively, these observations suggest two distinct mechanisms for how the activated SHP-2 mutants induce SIRPα and PZR hypertyrosyl phosphorylation.

Enhanced ERK Activation in Response to Adhesion of Ptpn11(D61G) Fibroblasts—SIRPα plays a role in cytoskeletal reorganization and migration (49, 53). Similarly, PZR has been shown to be involved in fibronectin-mediated cell migration (54). Because we have provided evidence that SIRPα and PZR are the two major hypertyrosyl-phosphorylated proteins associated with SHP-2 in *Ptpn11*$^{D61G/+}$ embryos, we hypothesized that MEFs derived from *Ptpn11*$^{D61G/D61G}$ embryos (D61G MEFs) might display defects in cell migration, adhesion, and/or adhesion-mediated signaling. To test these possibilities we used MEFs from *Ptpn11*$^{D61G/D61G}$ knock-in mice (18). We first determined

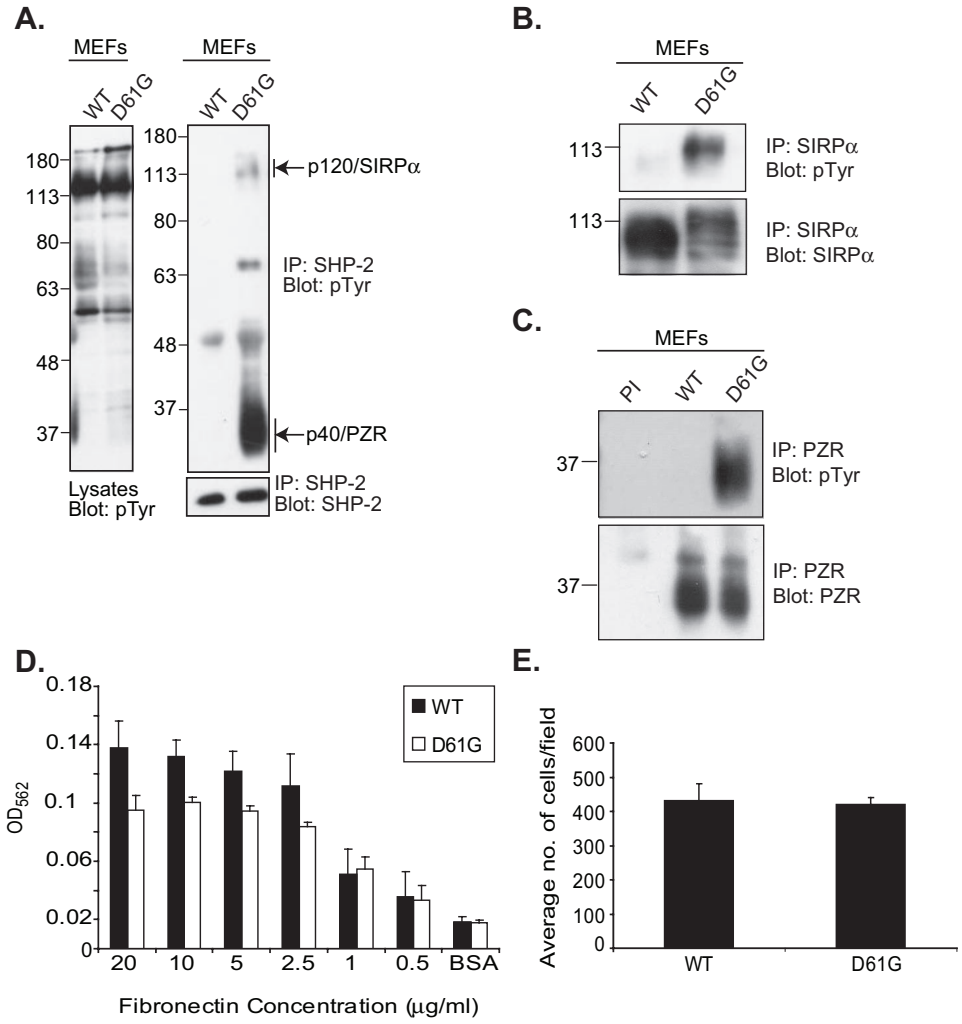

FIGURE 7. **Increased SIRPα and PZR tyrosyl phosphorylation but unaltered adhesion and migration in D61G MEFs.** *A,* cell lysates derived from WT and D61G MEFs were immunoblotted with anti-Tyr(P) (*pTyr*) antibodies (*left panel*) and were then subjected to immunoprecipitation (*IP*) with anti-SHP-2 antibodies, and immune complexes were immunoblotted with anti-Tyr(P) antibodies (*right panel*). *B,* cell lysates from *A* were subjected to immunoprecipitation with anti-SIRPα antibodies and immune complexes were immunoblotted with anti-Tyr(P) (*upper panel*) or anti-SIRPα (*lower panel*) antibodies. *C,* cell lysates from *A* were subjected to immunoprecipitation with anti-PZR antibodies, and immune complexes were immunoblotted with anti-Tyr(P) (*upper panel*) or anti-PZR (*lower panel*) antibodies. *D,* WT and D61G MEFs were re-plated onto fibronectin-coated wells, and attached cells were fixed and stained with 0.5% crystal violet solution, and OD_{562} was measured. *E,* WT and D61G MEFs were re-plated onto fibronectin-coated membranes, and transwell migration assays were performed. The results in *D* and *E* are representative of the mean ± S.E. from four and three separate experiments, respectively.

whether SIRPα and PZR were hypertyrosyl-phosphorylated and bound increased levels of SHP-2 (D61G). As shown previously, SHP-2 (D61G) co-precipitated with tyrosyl-phosphorylated p120/SIRPα and p40/PZR proteins (Fig. 7*A*), and SIRPα was hypertyrosyl-phosphorylated in D61G MEFs as compared with WT MEFs (Fig. 7*B*). Similarly, PZR was hypertyrosyl-phosphorylated in D61G MEFs as compared with WT MEFs (Fig. 7*C*). Next, we determined whether there are differences in extracellular matrix-mediated adhesion and migration between D61G and WT MEFs. We detected a slight reduction in fibronectin-mediated adhesion in D61G MEFs as compared with WT MEFs (Fig. 7*D*). Using fibronectin as an extracellular matrix substrate, we tested whether the D61G MEFs exhibited migratory defects. We found no detectable differences in migration as quantified in a transwell migration assay between WT and D61G MEFs (Fig. 7*E*).

SIRPα is involved in both positive and negative signaling effects to ERK in response to growth factors (42, 49, 55), although in response to adhesion-mediated integrin engagement SIRPα exerts a positive signaling effect on ERK (31). With regard to PZR, its role in ERK signaling has yet to be fully defined. Because NS-mediated signaling is proposed to involve enhanced Ras-ERK activation, we tested whether fibroblasts derived from the *Ptpn11*$^{D61G/D61G}$ knock-in mice might exhibit enhanced adhesion-dependent activation of ERK and whether SIRPα and/or PZR contribute to this effect.

First, we determined whether fibronectin-mediated ERK activation was enhanced in D61G MEFs in response to adhesion. D61G MEFs when re-plated onto fibronectin displayed a sustained activation of ERK, whereas ERK activation was more transient in WT MEFs (Fig. 8*A*). These results demonstrated that the activated D61G SHP-2 mutant enhances adhesion-mediated ERK activation. Our working hypothesis predicts that the increased SIRPα-D61G SHP-2 and/or PZR-D61G SHP-2 complex formation contributes to the sustained activation of ERK in response to adhesion-dependent signaling. Therefore, we tested whether down-regulating SIRPα expression attenuates the sustained activation of ERK in response to adhesion in D61G MEFs. We used siRNA to SIRPα to knock down its expression in D61G MEFs. As compared with nontargeting siRNA, transfection of SIRPα siRNA into D61G cells resulted in a substantial decrease in SIRPα expression (Fig. 8*B*). When we compared the kinetics of ERK activation in D61G MEFs following plating onto fibronectin, we found that siRNA SIRPα-treated D61G MEFs exhibited an attenuation of ERK activation as compared with nontargeting siRNA-treated controls (Fig. 8*B*). These results suggest that SIRPα and consequently increased plasma membrane association of SHP-2 D61G with SIRPα contribute to the enhanced activation of ERK in response to adhesion. To determine whether PZR plays a role in enhanced ERK activation in D61G MEFs in response to adhesion, we used siRNA to PZR to knock down its expression in D61G MEFs. As shown in Fig. 8*C*, we were able to eliminate its expression by more than 90%. When

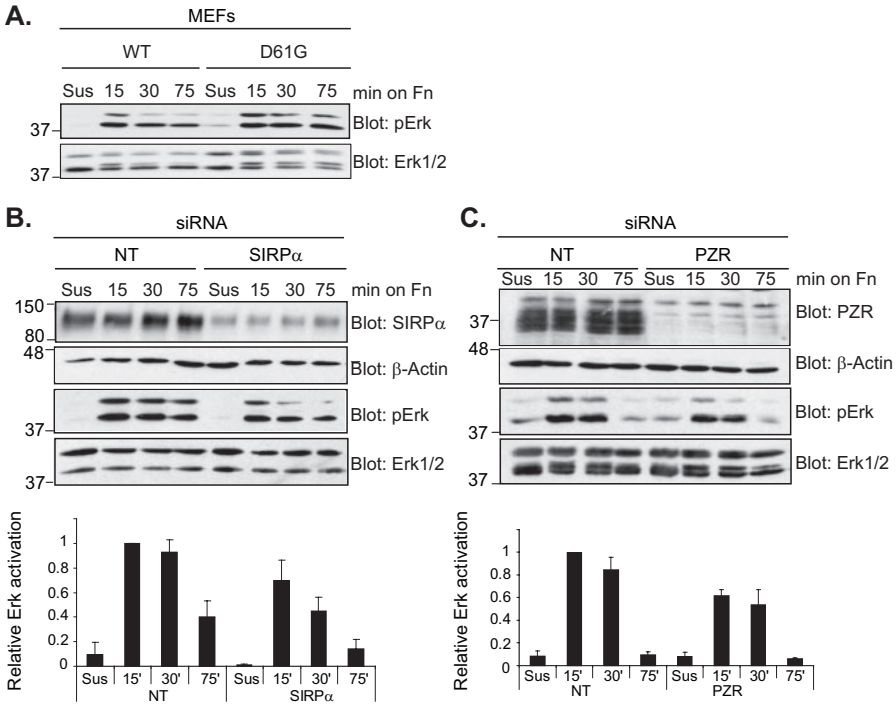

FIGURE 8. **Effects of SIRPα and PZR on enhanced adhesion-mediated ERK activation in D61G MEFs.** *A,* WT and D61G MEFs were serum-deprived, trypsinized, and were either maintained in suspension (*Sus*) or were re-plated onto fibronectin (*Fn*)-coated Petri dishes for the indicated times. Cell lysates were immunoblotted with anti-phospho-ERK1/2 (*upper panel*) and ERK1/2 (*lower panel*) antibodies. *B,* D61G MEFs were transiently transfected with either the control nontargeting (*NT*) siRNA or SIRPα siRNA. Transfected cells were serum-deprived, trypsinized, and either maintained in suspension (*Sus*) or re-plated onto fibronectin (*Fn*)-coated Petri dishes for the indicated times. Lysates were immunoblotted with anti-SIRPα, anti-β-actin, anti-phospho-ERK1/2, and ERK1/2 antibodies as indicated. *Graph* represents the mean ± S.E. densitometric analysis of relative ERK activation (pERK normalized to ERK) obtained from five separate experiments. *C,* D61G MEFs were transiently transfected with either the control nontargeting (*NT*) siRNA or PZR siRNA. Transfected cells were treated as indicated in (*B*). Lysates were immunoblotted with anti-PZR, anti-β-actin, anti-phospho-ERK1/2, and ERK1/2 antibodies as indicated. *Graph* represents the mean ± S.E. densitometric analysis of relative ERK activation (pERK normalized to ERK) obtained from three separate experiments.

we determined the kinetics of ERK activation in siRNA PZR-treated D61G MEFs following plating onto fibronectin, there was a moderate but consistent reduction of adhesion-dependent ERK activation as compared with the control treated cells (Fig. 8*C*). Together, these data demonstrate that increased association of SIRPα with SHP-2 D61G, and to a lesser extent with PZR, contributes to enhanced adhesion-mediated ERK signaling.

DISCUSSION

SHP-2 directs downstream signaling through its interactions with receptors, adaptor molecules, and transmembrane glycoproteins (1). In this regard, the effects of disease-associated SHP-2 signaling are likely to invoke similar requirements to promote aberrant signaling. Whereas the identity of some of these interacting proteins such as Gab-1 (17, 18) and Gab-2 (19, 33) has been elucidated, the pathophysiological targets of SHP-2 *in vivo* remain unknown. Here we identify the transmembrane glycoproteins SIRPα and PZR as hypertyrosyl-phosphorylated NS-associated SHP-2 mutant-interacting proteins during embryogenesis in a mouse model of NS. We show that SIRPα contributes to the enhanced ERK activation in D61G MEFs in response to adhesion. These data suggest that enhanced recruitment of NS-associated SHP-2 mutants to SIRPα and PZR during embryogenesis might contribute to enhanced ERK activation in response to extracellular matrix signals. Many developmental processes such as heart morphogenesis, neurogenesis, and vasculogenesis require the precise regulation of adhesion-dependent signals (56). Because NS patients exhibit complex cardiovascular defects and mental retardation, it is therefore conceivable that these defects might arise, at least in part, through promiscuous adhesion-dependent signaling mediated by activated SHP-2 mutants.

We identified PZR as a hypertyrosyl-phosphorylated protein in cells expressing activated SHP-2 mutants and during embryogenesis in the NS knock-in mouse model. The function of PZR still remains unclear, although our data suggest a potential role for PZR in adhesion-dependent signaling because PZR becomes inducibly tyrosyl-phosphorylated upon plating cells onto fibronectin, yet it fails to do so in response to growth factors. In support of these observations, it has been proposed that PZR is involved in the regulation of cell motility (54). However, we have been unable to observe such effects upon overexpression of PZR in either myoblasts or endothelial cells (data not shown). It is clear that additional work is needed before the function of PZR is fully elucidated. Nevertheless, our experiments are consistent with the idea that PZR might serve as an adhesion-regulated signaling molecule. It is not unreasonable to speculate that PZR tyrosyl phosphorylation and association with SHP-2 may play a role in adhesion-mediated signaling and that hypertyrosyl phosphorylation of PZR by NS/leukemia-associated SHP-2 mutants results in dysregulated extracellular matrix-dependent signaling. Consistent with this, we observe a moderate attenuation of adhesion-dependent ERK activation in PZR siRNA-treated D61G cells. These results suggest that PZR might only play a minor role in enhanced adhesion-dependent ERK activation. Further work will be required to identify the major pathway through which PZR signals.

Unlike PZR, the function and mechanisms of action of SIRPα are more defined. SIRPα becomes tyrosyl-phosphorylated and associates with SHP-2 in response to a variety of stimuli, including growth factors and extracellular matrix engagement (31, 43). In most cases it appears that tyrosyl phosphorylation of the ITIMs within the cytoplasmic tail of SIRPα are required for signaling. For example, overexpression of wild-type SIRPα leads to increased cell migration, whereas overexpression of the tyrosine phosphorylation site mutant has no effect (53). More-

over, a role for the cytoplasmic domain in general, has been provided using fibroblasts lacking the SIRPα cytoplasmic domain. These cells display increased focal adhesions, actin stress fibers, and migration defects (49). Therefore, our observation that SIRPα becomes hypertyrosyl-phosphorylated upon expression of the activated SHP-2 mutants suggests that downstream signaling from SIRPα is likely to be altered. Although we were unable to detect major differences in either cell adhesion and migration in D61G MEFs, we did observe that siRNA-mediated down-regulation of SIRPα expression decreases ERK activation in D61G MEFs in response to adhesion. These observations suggest that SIRPα contributes to SHP-2 D61G mutant-induced enhanced ERK activation in response to adhesion. However, we cannot exclude the possibility that other SIRPα-interacting proteins also participate in ERK activation.

How do activated SHP-2 mutants lead to hypertyrosyl phosphorylation of these target proteins? We initially hypothesized that the activated SHP-2 mutants stimulate a tyrosine kinase that subsequently phosphorylates SIRPα and PZR. Several studies have shown that SHP-2 functions upstream of the SFKs; moreover, both SIRPα and PZR are targets for phosphorylation by c-Src (30, 31, 57). Thus, c-Src is an attractive tyrosine kinase that could mediate both SIRPα and PZR tyrosyl phosphorylation by the activated SHP-2 mutants. When we examined c-Src activation, no major differences were detected between WT and *Ptpn11*$^{D61G/+}$ embryos under conditions in which both SIRPα and PZR were hypertyrosyl-phosphorylated. These results suggest that c-Src is unlikely to be a major target of SHP-2 that mediates SIRPα and PZR hypertyrosyl phosphorylation in this mouse model of NS at this stage of embryogenesis. However, we cannot exclude the possibility that c-Src becomes activated by the NS-associated SHP-2 mutant in a tissue-specific manner similar to that observed for ERK (18).

To further examine the mechanism by which activated SHP-2 mutants lead to hypertyrosyl phosphorylation of SIRPα and PZR, we determined whether the catalytic activity of the activated SHP-2 mutant is required for hypertyrosyl phosphorylation of these target proteins. Both SIRPα and PZR are hypertyrosyl-phosphorylated in the presence of the E76A/R465M SHP-2 mutant that represents an open conformation/catalytically inactive nonsubstrate-trapping mutant of SHP-2. The activated SHP-2 mutants are predicted to be in an open conformation even in the absence of any ligand (14, 15, 20). Therefore, it is conceivable that the SH2 domains of the activated SHP-2 mutants bind and protect their target proteins from dephosphorylation. Indeed, we found that hypertyrosyl phosphorylation of SIRPα occurred upon expression of the SH2 domains alone. The simplest interpretation of these results is that the SH2 domains of SHP-2 protect SIRPα from dephosphorylation. Although there are other possibilities, such as the SH2 domains of SHP-2 activating a tyrosine kinase that phosphorylates SIRPα, there is no evidence to support a positive signaling effect of the SH2 domains of SHP-2 alone. Hence, we favor the model that the SH2 domains of the activated SHP-2 mutants protect select phosphotyrosyl sites from dephosphorylation. In contrast, expression of the SH2 domains of SHP-2 alone blocked PZR tyrosyl phosphorylation. These results demonstrate that PZR hypertyrosyl phosphorylation does not occur as a result of a protection mechanism by the SH2 domains of SHP-2. We propose that the SH2 domains of SHP-2 acts as a dominant-negative (26, 52), thereby preventing activation and/or recruitment of a tyrosine kinase that phosphorylates PZR. Even though the identity of this putative tyrosine kinase is unknown, our data suggest that it is unlikely to be either Src, Yes, or Fyn. The possibility that other Src family kinase members are involved in PZR tyrosyl phosphorylation has yet to be formerly ruled out. Altogether, our results demonstrate that the activated mutants of SHP-2 lead to hypertyrosyl phosphorylation of SIRPα and PZR by distinct mechanisms.

In summary, we have identified that activated SHP-2 mutants in cultured cells and in a mouse model of NS cause hypertyrosyl phosphorylation of SIRPα and PZR and increased SHP-2 association. Our results imply that NS/leukemia-associated SHP-2 mutants engage extracellular matrix signals resulting in their increased recruitment to the plasma membrane via SIRPα and PZR, which may then function to enhance ERK signaling.

Acknowledgments—We thank Dr. Benjamin Neel for providing the D61G knock-in mice and Dr. Joe Zhao for PZR reagents.

REFERENCES

1. Neel, B. G., Gu, H., and Pao, L. (2003) *Trends Biochem. Sci.* **28,** 284–293
2. Feng, G. S. (1999) *Exp. Cell Res.* **253,** 47–54
3. Tiganis, T., and Bennett, A. M. (2007) *Biochem. J.* **402,** 1–15
4. Saxton, T. M., Henkemeyer, M., Gasca, S., Shen, R., Rossi, D. J., Shalaby, F., Feng, G. S., and Pawson, T. (1997) *EMBO J.* **16,** 2352–2364
5. Yang, W., Klaman, L. D., Chen, B., Araki, T., Harada, H., Thomas, S. M., George, E. L., and Neel, B. G. (2006) *Dev. Cell* **10,** 1–11
6. Saxton, T. M., Ciruna, B. G., Holmyard, D., Kulkarni, S., Harpal, K., Rossant, J., and Pawson, T. (2000) *Nat. Genet.* **24,** 420–423
7. Chen, B., Bronson, R. T., Klaman, L. D., Hampton, T. G., Wang, J., Green, P. J., Magnuson, T., Douglas, P. S., Morgan, J. P., and Neel, B. G. (2000) *Nat. Genet.* **24,** 296–299
8. Tartaglia, M., Mehler, E. L., Goldberg, R., Zampino, G., Brunner, H. G., Kremer, H., van der Burgt, I., Crosby, A. H., Ion, A., Jeffery, S., Kalidas, K., Patton, M. A., Kucherlapati, R. S., and Gelb, B. D. (2001) *Nat. Genet.* **29,** 465–468
9. Tartaglia, M., and Gelb, B. D. (2005) *Annu. Rev. Genomics Hum. Genet.* **6,** 45–68
10. Noonan, J. A. (1994) *Clin. Pediatr.* (*Phila.*) **33,** 548–555
11. Noonan, J. A. (1968) *Am. J. Dis. Child.* **116,** 373–380
12. Tartaglia, M., Kalidas, K., Shaw, A., Song, X., Musat, D. L., van der Burgt, I., Brunner, H. G., Bertola, D. R., Crosby, A., Ion, A., Kucherlapati, R. S., Jeffery, S., Patton, M. A., and Gelb, B. D. (2002) *Am. J. Hum. Genet.* **70,** 1555–1563
13. Musante, L., Kehl, H. G., Majewski, F., Meinecke, P., Schweiger, S., Gillessen-Kaesbach, G., Wieczorek, D., Hinkel, G. K., Tinschert, S., Hoeltzenbein, M., Ropers, H. H., and Kalscheuer, V. M. (2003) *Eur. J. Hum. Genet.* **11,** 201–206
14. Hof, P., Pluskey, S., Dhe-Pagganon, S., Eck, M. J., and Shoelson, S. E. (1998) *Cell* **92,** 441–450
15. O'Reilly, A., Pluskey, S., Shoelson, S. E., and Neel, B. G. (2000) *Mol. Cell. Biol.* **20,** 299–311
16. Tartaglia, M., Niemeyer, C. M., Fragale, A., Song, X., Buechner, J., Jung, A., Hahlen, K., Hasle, H., Licht, J. D., and Gelb, B. D. (2003) *Nat. Genet.* **34,** 148–150
17. Fragale, A., Tartaglia, M., Wu, J., and Gelb, B. D. (2004) *Hum. Mutat.* **23,** 267–277
18. Araki, T., Mohi, M. G., Ismat, F. A., Bronson, R. T., Williams, I. R., Kutok, J. L., Yang, W., Pao, L. I., Gilliland, D. G., Epstein, J. A., and Neel, B. G.

(2004) *Nat. Med.* **10,** 849–857
19. Mohi, M. G., Williams, I. R., Dearolf, C. R., Chan, G., Kutok, J. L., Cohen, S., Morgan, K., Boulton, C., Shigematsu, H., Keilhack, H., Akashi, K., Gilliland, D. G., and Neel, B. G. (2005) *Cancer Cell* **7,** 179–191
20. Keilhack, H., David, F. S., McGregor, M., Cantley, L. C., and Neel, B. G. (2005) *J. Biol. Chem.* **280,** 30984–30993
21. Zhang, S. Q., Yang, W., Kontaridis, M. I., Bivona, T. G., Wen, G., Araki, T., Luo, J., Thompson, J. A., Schraven, B. L., Philips, M. R., and Neel, B. G. (2004) *Mol. Cell* **13,** 341–355
22. Ren, Y., Meng, S., Mei, L., Zhao, Z. J., Jove, R., and Wu, J. (2004) *J. Biol. Chem.* **279,** 8497–8505
23. Fornaro, M., Burch, P. M., Yang, W., Zhang, L., Hamilton, C. E., Kim, J. H., Neel, B. G., and Bennett, A. M. (2006) *J. Cell Biol.* **175,** 87–97
24. Noguchi, T., Matozaki, T., Horita, K., Fujioka, Y., and Kasuga, M. (1994) *Mol. Cell. Biol.* **14,** 6674–6682
25. Milarski, K. L., and Saltiel, A. R. (1994) *J. Biol. Chem.* **269,** 21239–21243
26. Bennett, A. M., Hausdorff, S. F., O'Reilly, A. M., Freeman, R. M., and Neel, B. G. (1996) *Mol. Cell. Biol.* **16,** 1189–1202
27. Zito, C. I., Kontaridis, M. I., Fornaro, M., Feng, G. S., and Bennett, A. M. (2004) *J. Cell. Physiol.* **199,** 227–236
28. Wu, C. J., O'Rourke, D. M., Feng, G. S., Johnson, G. R., Wang, Q., and Greene, M. I. (2001) *Oncogene* **20,** 6018–6025
29. Zhang, S. Q., Tsiaras, W. G., Araki, T., Wen, G., Minichiello, L., Klein, R., and Neel, B. G. (2002) *Mol. Cell. Biol.* **22,** 4062–4072
30. Tsuda, M., Matozaki, T., Fukunaga, K., Fujioka, Y., Imamoto, A., Noguchi, T., Takada, T., Yamao, T., Takeda, H., Ochi, F., Yamamoto, T., and Kasuga, M. (1998) *J. Biol. Chem.* **273,** 13223–13229
31. Oh, E. S., Gu, H., Saxton, T. M., Timms, J. F., Hausdorff, S., Frevert, E. U., Kahn, B. B., Pawson, T., Neel, B. G., and Thomas, S. M. (1999) *Mol. Cell. Biol.* **19,** 3205–3215
32. Krenz, M., Yutzey, K. E., and Robbins, J. (2005) *Circ. Res.* **97,** 813–820
33. Yu, W.-M., Daino, H., Chen, J., Bunting, K. D., and Qu, C.-K. (2006) *J. Biol. Chem.* **281,** 5426–5434
34. Chan, R. J., Leedy, M. B., Munugalavadla, V., Voorhorst, C. S., Li, Y., Yu, M., and Kapur, R. (2005) *Blood* **105,** 3737–3742
35. Niihori, T., Aoki, Y., Ohashi, H., Kurosawa, K., Kondoh, T., Ishikiriyama, S., Kawame, H., Kamasaki, H., Yamanaka, T., Takada, F., Nishio, K., Sakurai, M., Tamai, H., Nagashima, T., Suzuki, Y., Kure, S., Fujii, K., Imaizumi, M., and Matsubara, Y. (2005) *J. Hum. Genet.* **50,** 192–202
36. Loh, M. L., Vattikuti, S., Schubbert, S., Reynolds, M. G., Carlson, E., Lieuw, K. H., Cheng, J. W., Lee, C. M., Stokoe, D., Bonifas, J. M., Curtiss, N. P., Gotlib, J., Meshinchi, S., Le Beau, M. M., Emanuel, P. D., and Shannon, K. M. (2004) *Blood* **103,** 2325–2331
37. Uhlen, P., Burch, P. M., Zito, C. I., Estrada, M., Ehrlich, B. E., and Bennett, A. M. (2006) *Proc. Natl. Acad. Sci. U. S. A.* **103,** 2160–2165
38. Kontaridis, M. I., Liu, X., Zhang, L., and Bennett, A. M. (2002) *Mol. Cell. Biol.* **22,** 3875–3891
39. Tartaglia, M., and Gelb, B. D. (2005) *Eur. J. Med. Genet.* **48,** 81–96
40. Bentires-Alj, M., Paez, J. G., David, F. S., Keilhack, H., Halmos, B., Naoki, K., Maris, J. M., Richardson, A., Bardelli, A., Sugarbaker, D. J., Richards, W. G., Du, J., Girard, L., Minna, J. D., Loh, M. L., Fisher, D. E., Velculescu, V. E., Vogelstein, B., Meyerson, M., Sellers, W. R., and Neel, B. G. (2004) *Cancer Res.* **64,** 8816–8820
41. Kontaridis, M. I., Liu, X., Zhang, L., and Bennett, A. M. (2001) *J. Cell Sci.* **114,** 2187–2198
42. Kharitonenkov, A., Chen, Z., Sures, I., Wang, H., Schilling, J., and Ullrich, A. (1997) *Nature* **386,** 181–186
43. Fujioka, Y., Matozaki, T., Noguchi, T., Iwamatsu, A., Yamao, T., Takahashi, N., Tsuda, M., Takada, T., and Kasuga, M. (1996) *Mol. Cell. Biol.* **16,** 6887–6899
44. Timms, J. F., Swanson, K. D., Marie-Cardine, A., Raab, M., Rudd, C. E., Schraven, B., and Neel, B. G. (1999) *Curr. Biol.* **9,** 927–930
45. Oshima, K., Ruhul Amin, A. R. M., Suzuki, A., Hamaguchi, M., and Matsuda, S. (2002) *FEBS Lett.* **519,** 1–7
46. Barclay, A. N., and Brown, M. H. (2006) *Nat. Rev. Immunol.* **6,** 457–464
47. Noguchi, T., Matozaki, T., Fujioka, Y., Yamao, T., Tsuda, M., Takada, T., and Kasuga, M. (1996) *J. Biol. Chem.* **271,** 27652–27658
48. van den Berg, T. K., van Beek, E. M., Buhring, H. J., Colonna, M., Hamaguchi, M., Howard, C. J., Kasuga, M., Liu, Y., Matozaki, T., Neel, B. G., Parkos, C. A., Sano, S., Vignery, A., Vivier, E., Wright, M., Zawatzky, R., and Barclay, A. N. (2005) *J. Immunol.* **175,** 7788–7789
49. Inagaki, K., Yamao, T., Noguchi, T., Matozaki, T., Fukunaga, K., Takada, T., Hosooka, T., Akira, S., and Kasuga, M. (2000) *EMBO J.* **19,** 6721–6731
50. Zhao, Z. J., and Zhao, R. (1998) *J. Biol. Chem.* **273,** 29367–29372
51. Zhao, R., and Zhao, Z. J. (2000) *J. Biol. Chem.* **275,** 5453–5459
52. Hausdorff, S. F., Bennett, A. M., Neel, B. G., and Birnbaum, M. J. (1995) *J. Biol. Chem.* **270,** 12965–12968
53. Motegi, S., Okazawa, H., Ohnishi, H., Sato, R., Kaneko, Y., Kobayashi, H., Tomizawa, K., Ito, T., Honma, N., Buhring, H. J., Ishikawa, O., and Matozaki, T. (2003) *EMBO J.* **22,** 2634–2644
54. Zannettino, A. C., Roubelakis, M., Welldon, K. J., Jackson, D. E., Simmons, P. J., Bendall, L. J., Henniker, A., Harrison, K. L., Niutta, S., Bradstock, K. F., and Watt, S. M. (2003) *Biochem. J.* **370,** 537–549
55. Takada, T., Matozaki, T., Takeda, H., Fukunaga, K., Noguchi, T., Fujioka, Y., Okazaki, I., Tsuda, M., Yamao, T., Ochi, F., and Kasuga, M. (1998) *J. Biol. Chem.* **273,** 9234–9242
56. Thiery, J. P. (2003) *Curr. Opin. Genet. Dev.* **13,** 365–371
57. Zhao, R., Guerrah, A., Tang, H., and Zhao, Z. J. (2002) *J. Biol. Chem.* **277,** 7882–7888